PROF. GERRIT T.S. BEEMSTER (Orcid ID : 0000-0001-6014-053X)

Article type : Regular Manuscript

How grass keeps growing: an integrated analysis of hormonal cross-talk in the maize leaf growth zone

Dirk De Vos[1,2,*], Hilde Nelissen[3,4], Hamada AbdElgawad[1,5], Els Prinsen[1], Jan Broeckhove[2], Dirk Inzé[3,4], Gerrit T.S. Beemster[1,*]

[1]Laboratory for Integrated Plant Physiology Research (IMPRES), Department of Biology, University of Antwerp, 2020 Antwerp, Belgium

[2]Modeling Of Systems And Internet Communication (MOSAIC), Department of Mathematics and Informatics, University of Antwerp, 2020 Antwerp, Belgium

[3]Department of Plant Biotechnology and Bioinformatics, Ghent University, 9052 Ghent, Belgium

[4]VIB Center for Plant Systems Biology, 9052 Ghent, Belgium

[5]Department of Botany and Microbiology, Faculty of Science, Beni-Suef University, Beni-Suef 62511, Egypt

ORCID: HN: 0000-0001-7494-1290; HAE: 0000-0001-9764-9006; EP: 0000-0003-4320-1585; DI: 0000-0002-3217-8407; GTSB: 0000-0001-6014-053X

*** Correspondence:**
Corresponding Authors

dirk.devos@uantwerpen.be, +32 3 265 34 21
gerrit.beemster@uantwerpen.be, +32 3 265 34 21

Received: *30 August 2019*
Accepted: *2 November 2019*

Keywords: modelling, simulation, maize, growth regulation, development.

ABSTRACT

- We studied the maize leaf to understand how long-distance signals, auxin and cytokinin, control leaf growth dynamics.
- We constructed a mathematical model describing the transport of these hormones along the leaf growth zone and their interaction with the local gibberellin (GA) metabolism in the control of cell division.
- Assuming gradually declining auxin and cytokinin supply at the leaf base, the model generated spatio-temporal hormone distribution and growth patterns that matched experimental data. At the cellular level, the model predicted a basal leaf growth due to cell division driven by auxin and cytokinin. Superimposed on this, GA synthesis regulated growth through the control of the size of the region of active cell division. The predicted hormone and cell length distributions closely matched experimental data.
- To correctly predict the leaf growth profiles and final organ size of lines with reduced or elevated GA production, the model required a signal proportional to the size of the emerged part of the leaf that inhibited the basal leaf growth driven by auxin and cytokinin. Excision and shading of the emerged part of the growing leaf allowed us to demonstrate that this signal exists and depends on the perception of light intensity.

Introduction

Successive leaves formed by young seedlings, although genetically identical and exposed to constant environmental conditions, reproducibly grow to strikingly different final sizes. This implies that the growth of individual leaves is balanced with the physiological status of the rest of the plant through long distance signalling, whereby the role of auxin and cytokinin balancing the growth of roots and shoots is a classic example (Hopkins and Hüner, 2008). The role of these and other phytohormones in organ growth regulation is probably best studied in the primary roots of *Arabidopsis thaliana*, where an auxin maximum and gradient at the root tip guides root growth (Grieneisen et al., 2007; Swarup et al., 2005) and works antagonistically with cytokinin to control the localization of cell division at the root tip and expansion in a region directly shootward from the division zone (Beemster and Baskin, 2000; Perilli et al., 2012; De Vos et al., 2014; Moore et al., 2015). Superimposed on the role of auxin and cytokinin, gibberellins play a key role, determining the location of the boundary between the division and expansion zone (Ubeda-Tomas et al., 2008; Achard et al., 2009).

A similar linear organisation of developmental zones is also present in the growing maize leaf (Avramova et al., 2015b). At the base a zone with cell division precedes a zone with cell expansion without division and a mature zone, in which growth has ceased and cell differentiation is finalized. Since the transition between the division zone (DZ) and the expansion/elongation zone (EZ) is not abrupt, the term transition zone (TZ) is used for the zone with decreasing cell proliferation and increasing expansion (Verbelen et al., 2006). The size of these zones in the maize leaf facilitate measuring the dynamics of the plant hormones and transcripts of genes encoding associated biosynthetic enzymes, transport and downstream responses across the spatial gradient (Avramova et al., 2015b). Mass spectrometry analyses demonstrated that hormone gradients exist along the growth zone, with basipetally increasing concentration gradients of auxins and cytokinins and a local accumulation at the transition zone of bioactive gibberellins (GAs; Nelissen et al., 2012). The growth of the GA biosynthesis defective *dwarf3* mutant is impaired due to a strongly reduced DZ size, whereas overproduction of GAs increases the DZ size. This demonstrated a key role for GA in leaf growth regulation trough the spatial control of cell proliferation (Nelissen et al., 2012). DELLA proteins belonging to the GRAS family of transcription factors (Bolle, 2004) play a key role in GA signal transduction (Pacifici et al., 2015). The *dwarf8* mutant, defective in GA signalling by DELLA stabilization, phenocopies *dwarf3*, suggesting that the spatial control mechanism by GA in the maize leaf growth zone operates in a DELLA-dependent way (Nelissen et al., 2012).

Although the role of individual hormones in organ growth control is well documented, how they interactively integrate long distance signals in the control of cell division and expansion is far from clear (Ubeda-Tomás et al., 2012). To address this issue, we investigated if we could construct a computational model for hormonal regulation of maize leaf growth, which integrates existing knowledge, empirically measured hormone levels and transcript data with quantitative cellular and macroscopic leaf growth data. The maize leaf offers an ideal system to study growth control, since, the growth process of grass leaves can be subdivided in three stages: Prior to emergence primordial growth is exponential (Beemster and Masle, 1996). After emergence from the whorl of older leaves, growth of leaves of *Gramineae* during the first days after emergence can be assumed steady-state under stable conditions, enabling comparative cellular growth analysis (Rymen et al., 2010), although it is constantly varying under natural conditions (Caldeira et al., 2014). After the linear phase, leaf growth rates progressively decline (Nelissen *et al.*, 2016). Next to growth rate, the duration of growth is a crucial factor determining final leaf size (Baute *et al.*, 2015; Sun *et al.*, 2017).

To investigate the control mechanisms involved, we built a maize leaf growth model driven by long-distance signals (auxin and cytokinin) supplied at the base of the leaf, generating a spatial gradient by the combined effect of diffusion, movement, dilution by cell growth and catabolism. Local concentrations of auxin and cytokinin directly drive the cell cycle, but also indirectly through

crosstalk with GA. Based on appropriate auxin and cytokinin influx functions, this basal model was sufficient to simulate wild-type leaf growth dynamics. However, studies of mutants with perturbed GA signalling and growth rates suggested additional control through a leaf size feedback mechanism. Experimental perturbations allowed us to prove the existence of a signal from the emerged, mature part of the leaf and its dependence on light interception.

Materials and methods

Model Development

Because maize leaves predominantly grow longitudinally, with limited expansion in the lateral and anticlinal direction, we used the modelling software VPTissue (De Vos et al., 2017) to represent a section of the leaf by a dynamic lattice or mesh (see Methods S1, Fig. S1) that is restrained to only grow longitudinally. An elastic force in the cell walls ensures that a turgor pressure is maintained that drives one-directional growth. To describe transport, a passive (concentration dependent) permeation process in combination with cell/tissue movement was used in combination with a concentration dependent decay to reproduce the available experimental hormone profiles. Hence, the more complex processes that may be involved including facilitated or active transport (e.g. PIN mediated: Merks et al., 2007; Balzan et al., 2014; Yue et al., 2015) were not included in the model(s) of this study.

Rather than single compounds, the variables represent functionally related families of bio-chemicals, metabolites and proteins (cf. Methods S1 for details). We have opted to use such 'aggregate' variables to allow focussing on higher order regulatory properties of hormones in plant growth regulation. Apart from the variables, the models are also simplified in terms of their interactions. Hormone (or hormone family) activity depends on complex signalling/expression pathways. The kinetic expressions used here serve as their proxy and the kinetic constants in the expressions are therefore 'apparent' and represent the relative influence of the respective variables and not a single isolated interaction.

We hypothesise that the spatial gradient of these regulators is determined by long range communication, related to the physiological state of the plant, arriving at the leaf base. Import of AUX and CK into the system are captured by equation(s) (Eqs. 1-4), containing a progressively decreasing supply term if the time $t < t_{sup}$ (the duration that auxin and cytokinin are supplied at the base of the leaf) for the bottom row cells of the cellular mesh (Notes S1):

$$\frac{d[CK]}{dt} = \frac{k_{sCK}}{area} \cdot \left(1 - \frac{t}{t_{\sup}}\right) - k_{dCK} \cdot CK + \frac{P_{CK}}{area} \cdot \sum_i l_i \cdot \Delta c_{CK} \quad \text{(Eq. 1)}$$

$$\frac{d[AUX]}{dt} = \frac{k_{sAUX}}{area} \cdot \left(1 - \frac{t}{t_{\sup}}\right) - k_{dAUX} \cdot [AUX] + \frac{P_{AUX}}{area} \cdot \sum_i l_i \cdot \Delta c_{AUX} \quad \text{(Eq. 2)}$$

If $t > t_{sup}$, small constant production terms remain, similar to what all non-basally located model cells have (Notes S1 for more details on the model equations):

$$\frac{d[CK]}{dt} = \frac{k_{sCKp}}{area} - k_{dCK} \cdot [CK] + \frac{P_{CK}}{area} \cdot \sum_i l_i \cdot \Delta c_{CK} \quad \text{(Eq. 3)}$$

$$\frac{d[AUX]}{dt} = \frac{k_{sAUXp}}{area} - k_{dAUX} \cdot [AUX] + \frac{P_{AUX}}{area} \cdot \sum_i l_i \cdot \Delta c_{AUX} \quad \text{(Eq. 4)}$$

The last term in Eqs. 1-4 represents cell-to-cell transport driven by concentration differences between neighbouring cells and was included to produce the spatial hormone profiles, for which experimental data were available (Nelissen et al., 2012). This effectively ignores the potential effect of cell length dependent intracellular transport rates on those profiles. We therefore derived a

kinetic expression for cell-length dependent permeation and applied it to our model to demonstrate that the role of increasing cell length (transport path length) along the growth axis is relatively small and can be safely neglected in this study (Notes S2).

Central in the model is the regulation of the zone of cell proliferation (division zone or 'DZ') as a function of a generic Cyclin Dependent Kinase (CDK) activity (Eq. 1). Above an arbitrary CDK concentration and cell size threshold, a cell divides into equally sized daughter cells by producing a new transversal cell wall (Methods S1, see Notes S1). Since cells do not typically divide in a synchronized way, random noise is added in the evaluation of the size threshold. Cells leaving the resulting division zone undergo increased cell expansion during a fixed time before growth arrest (maturation). In the model, two main CDK regulatory modules are proposed: a direct path of influence via auxins and cytokinins, and a gibberellin (GA) dependent pathway (Fig. 1). In accordance with existing knowledge, cross-talk occurs between both modules (Fig. 1: blue box). Auxin and cytokinin signals are known to be required for cell division (Perrot-Rechenmann, 2010; Stals and Inze, 2001) and to positively influence CDK activity (Hartig & Beck, 2006; Dudits et al., 2011). For the influence of GA on cell division we assume that it acts in a DELLA dependent way (Nelissen et al., 2012), with DELLAs restraining growth by controlling cell division (Xu et al., 2014) potentially directly influencing CDK activity (Claeys et al., 2012). Combined this leads to the following equation:

$$\frac{d[CDK]}{dt} = \left(k_{sCDK} + \frac{k_{sCDKp}}{K_{iDELLAp} + [DELLA]}\right) \cdot \left(\frac{[CK]}{K_{mCK} + [CK]}\right) \cdot \left(\frac{[AUX]}{K_{mAUX} + [AUX]}\right) - k_{dCDK} \cdot [CDK] \quad \text{(Eq. 5)}$$

Which expresses both DELLA independent and DELLA dependent CDK production terms via the first factor on the right-hand side, with the latter leading to inhibition at increasing DELLA concentrations. The second and third factor, respectively, confer a positive but saturating effect of cytokinin and auxin.

The GA pathway is represented in its most rudimentary form, by production of the principal active form GA1 and its inactive product GA8, that is subsequently degraded. Without an explicit substrate, production is assumed to be proportional to the activity of the biosynthetic complex. For the GA1 to GA8 conversion (Michaelis-Menten type) saturation kinetics were used to reproduce the available GA1/GA8 spatial data (cf. *Experimental data fitting*).

$$\frac{d[GA1]}{dt} = k_{GA203OX} \cdot [GA20,3OX] - k_{GA2OX} \cdot \frac{[GA2OX] \cdot [GA1]}{K_{mGA1} + [GA1]} - k_{dGA1} \cdot [GA1] + \frac{P_{GA1}}{area} \cdot \sum_i l_i \cdot \Delta c_{GA1} \quad \text{(Eq. 6)}$$

$$\frac{d[GA8]}{dt} = k_{GA2OX} \cdot \frac{[GA2OX] \cdot [GA1]}{K_{mGA1} + [GA1]} - k_{dGA8} \cdot [GA8] + \frac{P_{GA8}}{area} \cdot \sum_i l_i \cdot \Delta c_{GA8} \quad \text{(Eq. 7)}$$

A crucial aspect of our model is the dependence of GA1 regulation on the activities of the GA20OX, GA3OX and GA2OX enzymes (isoforms), for which transcript levels were reported (Nelissen et al., 2012), and can considered to be essential in control of the GA pathway in plants (Weiss and Ori, 2007; O'Neill et al., 2010). We assumed auxin and cytokinin to be the main factors determining spatial and temporal regulation of those enzymes, as expressed by Equations 8 and 9. They are based on known antagonism in the (transcriptional) effects –positive versus negative- of auxin on GA1 formation and breakdown, respectively (Weiss and Ori, 2007: O'Neill and Ross, 2002; Frigerio et al., 2006). Furthermore, a negative transcriptional influence of cytokinin on GA biosynthesis is included (Weiss and Ori, 2007; Fleishon et al., 2011). By adjusting the kinetic parameters of Eq. 8, a strong local inhibition (at the leaf base) by CK can be combined with a less confined activation by AUX. This can drive the generation of the GA20/3OX activity peaks important in producing the characteristic GA1 maximum. GA1 stimulates its own conversion to GA8 in a DELLA dependent way by de-repressing GA2OX (Zentella et al., 2007; Weston et al. 2008). The AUX dependent inhibition factor of Eq. 9 ensures that basal GA2OX concentrations are relatively lower than GA20/3OX, which explains the observed distal shift of the GA8 peak relative to the GA1 peak. The exponent '2' in Eqs. 8 and 9 are required to confer a strong input-output response typical for the kinetics of signalling pathways or allosterically regulated enzymes.

$$\frac{d[GA20,3OX]}{dt} = \frac{k_{sGA203OX}}{1+\left(\frac{K_{aAUX}}{[AUX]}\right)^2+\left(\frac{[CK]}{K_{iCK}}\right)^2} - k_{dGA203OX}\cdot[GA20,3OX] \quad \text{(Eq. 8)}$$

$$\frac{d[GA2OX]}{dt} = k_{sGA2OX} + \frac{k_{sGA2OXp}}{(K_{iDELLA}+[DELLA])\cdot\left(1+\left(\frac{[AUX]}{K_{iAUX}}\right)^2\right)} - k_{dGA2OX}\cdot[GA2OX] \quad \text{(Eq. 9)}$$

Finally, the dynamics of DELLA are determined by a constitutive production term and a proportional decay term with a constitutive and a GA1 concentration dependent component (Eq. 10).

$$\frac{d[DELLA]}{dt} = k_{sDELLA} - (k_{dDELLA} + k_{dDELLAp}\cdot[GA1])\cdot[DELLA] \quad \text{(Eq. 10)}$$

Implementing these reactions in the context of the cell growth and division module of the VPTissue software allowed us to simulate the dynamics of the growth process of an individual leaf from its inception as a small group of cells at the side of the shoot apical meristem to maturity (Fig. S1).

Extended model with negative feedback from the emerged part of the leaf

Eqs. 15-17 express those relations mathematically.

$$\frac{dCK}{dt} = k_{sCK}\cdot\frac{1}{\left(1+\frac{M}{K_{iM}}\right)} + k_{sCKp} - k_{dCK}\cdot CK \quad \text{(Eq. 15)}$$

$$\frac{dAUX}{dt} = k_{sAUX}\cdot\frac{1}{\left(1+\frac{M}{K_{iM}}\right)} + k_{sAUXp} - k_{dAUX}\cdot AUX \quad \text{(Eq. 16)}$$

$$\frac{dM}{dt} = k_{sM} - k_{dM}\cdot M \text{ , with } k_{sM} = 0\ k_{sM} = 0 \text{ if time since last division} < tEZ \quad \text{(Eq. 17)}$$

The source code for the described models is publicly available on https://bitbucket.org/ddevos/maize/src.

Experimental procedures

Plant growth conditions

Maize seedlings were grown in individual pots at 25/18 ºC, 300 µmol.m^{-2}s^{-1} Photosynthetically Active Radiation and 16h/8h day/night cycles. Soils were re-watered daily to a Soil Water Content (SWC) of 54%. Young maize leaves (leaf #5) were harvested at day 0, 4, 8, 12 and 16 after emergence from the whorl of older leaves. The first 1 cm from the leaf basis of harvested leaves was cut and stored at -80°C for hormonal measurements.

Hormones extraction and analysis

Homogenized plant material was extracted in methanol (80% (v/v) for 16 h at −20°C. Internal standards ([C_6^{13}] Phenyl-Indole-3-acetic Acid (100 pmol; Cambridge Isotope Laboratories Inc., Tewksbury, MA, USA,), 20 pmol of [$^2H_2$]GA1 (OlChemIm Ltd. Olomouc, Czech Republic), 20 pmol of [$^2H_2$]GA3 (OlChemIm), 20 pmol of [$^2H_2$]GA8 (OlChemIm), 20 pmol of [$^2H_2$]GA19 (OlChemIm), 10 pmol D5-*trans*-Zeatin (OlChemIm), 10 pmol D5-*trans*-Zeatin Riboside (OlChemIm), 10 pmol D6-N^6-isopentenyladenine (OlChemIm), 10 pmol D6-N^6-isopentenyladenosine (OlChemIm), 10 pmol D7-N^6-Benzyladenosine (OlChemIm) and 10 pmol D7-N^6-Benzyladenine (OlChemIm). were added. Pigments were removed on a C18 cartridge (Bond Elut C18 6 cc, 500 mg; Agilent) in 80% (v/v) methanol. The extract was diluted and acidified with formic acid (6%, v/v) and purified on an additional C18 cartridge. The hormones retained to the C18 cartridge were eluted by using diethyl ether. Samples extracts were dried and re-dissolved in 50 µL of 10% (v/v) methanol for liquid chromatography-mass spectrometry analysis of hormones. For more details about extraction and analyses see Fina et al., (2017).

Shading and removing the mature part of maize leaf

In this experiment, uniformed size and weight grains were surface sterilized using 35% (v/v) of commercial bleach for 30 min and rinsed several times with sterilized distilled water. Maize seedlings (20 per experiment) were grown in individual pots under controlled conditions (average temperature = 25, humidity = 35 %, with a 12h/12h day/night cycle). Pots were re-watered daily to 54% (SWC). The mature part of leaf four was shielded from light directly after its emergence with aluminium foil, transparent plastic foil or cloth sheath or cut on a daily base for 24 days after which the total leaf length was measured. For meristem measurements, samples harvested 3 days after leaf emergence and the size of the meristem zone of the leaves was estimated by locating the most distal mitosis in the cell files. Cell length and number in mature leaf were measured by light microscopy (Avramova et al., 2015a).

Results

Different types of molecular data are available on the regulation of the steady state growth of the maize leaf (Nelissen et al., 2012, Avramova et al., 2015a, Nelissen et al., 2018) and to integrate them in a mechanistic model of leaf growth regulation, we based ourselves on existing knowledge of hormonal interactions and cell cycle control. This allowed us to formulate a conceptual model scheme with 8 variables (Table 1) and 11 interactions (arrows) that describes the relations between long distance signals auxin and cytokinins supplied to the base of the growing leaf, localised gibberellin metabolism and the control exerted by these hormones on cell cycle progression summarized as CDK activity (Fig. 1). We implemented this molecular network and its link to cell level growth processes using the plant tissue growth modelling software VPTissue (De Vos et al., 2017). Because maize leaves predominantly grow longitudinally, we represented the leaf by a dynamic lattice or mesh (see Methods S1, Fig. S1) that is restrained to only grow longitudinally. An elastic force in the cell walls ensures that turgor is maintained and drives one-directional growth. To describe transport, passive (concentration dependent) permeation and cell/tissue movement was used in combination with a concentration dependent decay to reproduce the available experimentally obtained hormone profiles. Additional processes that may be involved, including facilitated or active transport (e.g. PIN mediated: Merks et al., 2007; Balzan et al., 2014; Yue et al., 2015) were not included in the model(s) of this study.

Simulation of auxin and cytokinin influx at the base of the leaf

Using this model, we first considered auxin (AUX) and cytokinin (CK) influx at the leaf base that provides the interface of the model with the rest of the plant. We assumed that due to the ongoing initiation and development of new leaves at the shoot apex, the supply of these hormones progressively decreases over time and that this would be reflected by gradually decreasing concentrations at the base of the leaf. Based on gradually declining AUX and CK influx, simulation by the model indeed produces

progressively decreasing auxin concentrations at the leaf base (Fig 2A). To test the validity of this assumption, we measured levels of the auxin Indole-3 Acetic Acid (IAA) and cytokinins (cZ, IPA, BAP, tZR, cZR, Fig. S2) in the basal 1 cm of the 5th leaf of B73 maize seedlings from their emergence till they stopped growing. Consistent with the model prediction, auxin and cytokinin concentrations at the base of the leaf decreased over time (Fig. 2A, B, S2) reflecting reduced import into the leaf base. Given the error bars on the experimental data, we attribute the more complex evolution of total cytokinin levels to the combined experimental noise of the individual molecules and consider the model to broadly capture the globally decreasing trend (Fig. 2B). We conclude that the boundary conditions for the model at the base of the leaf are therefore realistic and provide the basis for simulating the spatial gradients along the length of the leaf.

Simulation of hormone gradients along the leaf axis

Next, we tested the ability of the model to generate realistic hormone gradients along the leaf during the phase of steady state growth. Consistent with earlier measurements (Nelissen et al., 2012), we found that both auxin and cytokinin levels progressively decrease with increasing distance from the leaf base (Fig. 3A). Because cytokinin levels drop more steeply, the model transport parameters were set so that CK decreases more rapidly than AUX along the longitudinal axis (Fig. 3B). With these settings the model reproduced the experimental data, albeit with a sharper drop in CK and AUX at the transition between division and expansion zones. This is most likely due to non-synchronicity between transport processes and mechanical equilibration (time-scale separation) in the modelling framework. The model does not capture the occurrence of a more distal CK increase in experimental data (Fig. 3A). |This increase occurs in mature tissue and presumably not related to the regulation of cellular growth processes. Taken together, the global characteristics of the AUX and CK curves in the basal part of the leaf reproduce the experimental data and provide a basis to extend the model with GA interaction and biosynthesis modules (Fig. 1: Blue and Pink boxes) and compare its predictions with experimental data.

To this end, we measured the levels of the dominant active gibberellin isoform GA1 and its inactivated form GA8 along the leaf growth zone and determined the biochemical activity of the main enzymes GA3OX and GA2OX, controlling biosynthesis of GA1 and conversion to GA8, respectively. Consistent with our earlier findings (Nelissen et al., 2012), GA1 and GA8 levels in the wild type show a distinct peak around 1 cm from the base of the leaf and a slight shift of the GA8 peak to more distal positions, reflecting active breakdown of GA1 (Fig. 4A). The corresponding enzyme activities show a similar distribution, demonstrating that local biochemical activity largely determines the metabolite levels (Fig. 4B, C).

To better understand the functioning of the GA module, we also analysed the GA20OX-1 overexpression (UBI::GA20-OX-1) and *dwarf3* (defective in early GA biosynthesis) lines, in which the GA1 and GA8 peaks are strongly increased and absent, respectively (Fig. 4A; Nelissen et al., 2012). The peak of GA3OX enzyme activity is slightly elevated in UBI::GA20-OX-1 and shifted to more distal positions, whereas this increase and shift is much more prominent for the GA2OX activity (Fig. 4B,C).

To simulate the UBI::GA20-OX-1 and *dwarf3*, we assumed 3-fold higher GA1 production (kGA203OX = 30 min^{-1}) and 40-fold lower GA1 production (kGA203OX = 0.25 min^{-1}), respectively (parameters for the wild type 'master' model in Table S1). The model reproduces the peak positions and relative levels of GA1 and GA8 in wild type and overexpression line during steady-state growth (Fig. 4A,D). For UBI::GA20-OX-1 in contrast, this shift is particularly clear and closely linked to the broader GA3OX expression domain in this line (Fig. 4B), which is also reproduced by the model (Fig. 4E). GA1 causes activation of its own conversion in the form of GA2OX de-repression (Fig. 1), which explains the effects on measured and simulated levels, respectively (Fig. 4C,F). The predicted higher levels and shift of the GA2OX peak away from the base in UBI::GA20-OX-1 are reflected in the experimental data (Fig. 4C). The position however appears to be shifted more strongly in the experimental data, which could partly be explained by inability to detect the predicted sharp drop in the experimental data due to biological variation and the 0.5 cm

sampling size. The simulations do not accurately predict the peak height ratio between GA1 and GA8 observed in the over-expression line (Fig. 4A and D). The higher experimental peak ratio is in line with higher induction of GA2OX expression levels relative to the leaf base in the simulated compared to the predicted levels (Fig. 4C and F). The strong decrease in the levels of GA1 and GA8 in *dwarf 3* (Fig. 4A) are effectively reproduced by the model (Fig. 4D). Overall, these results show that the experimental spatial patterns of auxin, cytokinin and GA molecules involved in leaf growth regulation are effectively simulated with this model describing the influx of two of them (AUX and CK) at the leaf base, their transport and regulatory interactions with GA biosynthetic enzyme activities (Fig. 1).

Next to simulating the hormone distribution along the growth zone during steady state at 2 days after leaf emergence, we simulated these distributions at different stages during growth. The predictions indicate that AUX and CK gradients gradually retreat (Fig. 5A). The GA1 and 8 peaks in contrast are more stable, and the GA8 peak maintains a more distal position relative to that of GA1 (Fig. 5B; corresponding with the GA20/3Ox and GA2Ox enzyme activities Fig. S3). Finally, our predictions show that DELLA levels are suppressed at the leaf base until the GA1 peak disappears upon growth cessation (Fig. 5B).

Simulation of cellular growth characteristics

The ability of the model to simulate the molecular changes in a spatial-temporal manner, allowed us to evaluate cell level growth parameters to examine to what extent they explain leaf growth dynamics. The size of the proliferation or division zone (DZ) of the leaf is a key determinant of leaf elongation rate (LER) in grasses (Gázquez and Beemster, 2017; Fig. S3). Nelissen et al. (2012) hypothesized that the spatial concentration profile of active GA determines/modulates the transition from DZ to elongation zone (EZ) through increases in the GA1 peak height and/or location. We integrated this hypothesis in our model and calibrated the minimum CDK activity threshold for cell division, so that the location of the DZ-EZ transition coincides with the experimentally determined location during steady state growth. We also adapted the cellular growth rates in the DZ and EZ, and the duration of the expansion phase (Table S1), so that the final (mature) leaf length approximated values measured for WT. Setting the GA1 production rate constant to match the relative GA1 concentrations for overproduction and dwarf lines (Fig. 4A,D) yielded a characteristic sigmoidal growth and predictions of final leaf lengths (Fig. 6A) closely resembling experimental data (Nelissen et al., 2012). The corresponding simulated leaf elongation rate curves for the three lines with contrasting GA levels not only predict differences in LER, but also in timing of growth arrest (Fig. 6B). This difference in leaf elongation duration (LED) was however not observed *in vivo* (Nelissen et al., 2012).

While the spatial model is not at cellular resolution, it allows calculation of a cell length profile along the growth axis based on the relative size of the modelled cells. The predicted cell length curves are in accordance with experimental values (Nelissen et al., 2012): The dwarf and OE simulations yield basal and apical curve shifts coupled to a similar mature cell length (Fig. 7), as a consequence of different DZ sizes and similar cell expansion rates in the elongation zone.

Including feedback from the mature part of the leaf in the model

The inconsistency of the predicted effect of reduced and increased GA1 biosynthesis on the duration of leaf growth, suggests that differences between the investigated lines cannot be explained by a difference in GA-dependent regulation alone. It struck us that relative to the wild type, growth duration is underestimated in slow growing mutant and overestimated in the fast-growing GA overproducer. Hence, there is a positive correlation between growth and the inhibition that would be required to correct the growth profile. This suggested to us the involvement of a negative feedback between organ growth (or size) on the growth regulation. Diverse mechanisms can be proposed to explain why the slower growing *dwarf3* does not lose its growth signals as quickly as UBI::GA20-OX-1. For instance, the distance of external auxin sources such as the shoot apex (to the growing leaf) could play a

role. Alternatively, signals produced in the mature part of the leaf that negatively affect AUX and CK import or activity would achieve the same effect. Because in earlier studies we observed a negative feedback from mature to proliferating cells in *Arabidopsis* leaves (Andriankaja et al., 2012), we implemented this possibility as a new model variant. To this end we introduced a new variable (maturation factor 'M'), which is produced by cells that have stopped elongating ('mature' cells). M is transported passively and therefore diffuses from the distal parts of the leaf to the cells at its base. If the M concentration is high enough, the basal production/availability of AUX and CK is progressively inhibited or reduced. Since the amount of mature tissue gradually increases, the inhibitory effect will eventually reach a point at which hormone levels are so low that growth is no longer sustained and leaf growth arrests. Simulation results show that this mechanism produces very similar spatial hormone patterning (Fig. S4), while effectively adjusting the duration of the LER curve. Variation of the inhibitory strength (via 'KiM') results in different growth termination times, with weak inhibition (KiM=200) significantly extending the duration of leaf growth (Fig. 8).

Experimental Validation of a potential Feedback mechanism

To experimentally verify whether the mature part of emerged maize leaves can effectively inhibit growth at the leaf base (auto-inactivation), we first compared growth of the 4th leaf of B73 maize seedlings with that of seedlings from which the (mature, no longer growing) emerged part of leaf 4 was cut off at a daily basis and stored at 4 °C. The final leaf length of control plants was significant shorter than the length obtained by realigning all the cut pieces and measuring the total length (Fig. 9). To investigate if light exposure could play a role in auto-inactivation of leaf growth, we tested the effect of covering the emerged part of the leaf with aluminium foil. As expected, blocking light from the mature part of the leaf significantly ($p < 0.01$) increased its final length (Fig. 9), indicating that a light-dependent signal from distal leaf parts indeed provides a negative feedback on the growth processes at the leaf base.

To investigate the potential nature of the signal, we tested the effect of covering the leaf with aluminium foil, cutting the emerged mature part, reducing the light intensity with shade cloth and reducing evaporation with transparent plastic foil. Shade cloth reduced the amount of light reaching the leaf but does not affect the photoperiod or light spectrum. Nevertheless, leaves covered by shade cloth grew significantly longer (Fig. 10A), which excludes a phytochrome driven response. We tested the possibility that the signal is hydraulic, driven by evaporation from the emerged part of the leaf. However, covering the leaf with transparent plastic foil to reduce transpiration, did not significantly increase leaf length (Fig. 10A). This suggests that the signal is proportional to the amount of light received by the mature part of the leaf. We then investigated the cellular basis of the enhanced growth of covering or removing the mature part of the leaf and found that the growth stimulation was due to increased cell production (Fig. 10B), while mature cell size was not affected (Fig. 10C). The increased cell production could be explained by an increased size of the division zone (Fig. 10D). Therefore, our results are consistent with the involvement of a new feedback signal impinging on the regulation of cell division from the mature part of the leaf that is proportional to the amount of light it perceives.

Discussion

We developed a mathematical model describing the molecular and cellular basis of growth regulation at the base of the maize leaf. This model is driven by auxin and cytokinin supply from the rest of the plant at the base of the leaf. By diffusion, growth dilution and decay this influx determines spatio-temporal auxin and cytokinin gradients along the leaf. These two hormones directly stimulate CDK activity and thereby cell division, but also drive GA synthesis, that through a DELLA-mediated response, further stimulate cell division at longer distance from the leaf base. Finally, a feedback inhibition on auxin and cytokinin availability is included to explain similarity of duration of leaf growth in fast and slow growing GA mutants and increased growth in response to shading experiments.

Spatio-temporal modelling has become an established part of plant systems biology research (De Vos et al., 2012; Hodgman and Ajmera, 2015). Mathematical modelling and analysis offer the possibility to understand properties and behaviour of complex biological systems when simple logic falls short. Approaches can be distinguished depending on the type of variables and the rules or equations describing their behaviour. We built a spatio-temporal model of maize leaf growth based on a selected set of variables that represent crucial molecular factors evolving at the time-scale of hours to days. Although individual molecular process can involve intricate regulatory details (e.g. De Vos et al., 2004; 2007), we used simplified generic kinetic expressions combined in ordinary differential equations. Model abstraction and simplification reduced the number of parameters to optimize and kept simulation run times manageable, while providing a starting point for further model extension and refinement. Furthermore, we implemented a coarse-grained spatial representation of a maize leaf, starting from a regular grid, using the VPTissue simulation framework (De Vos et al., 2017). The stochastic nature of the underlying tissue mechanics algorithm requires averaging across multiple independent simulation runs for model analysis, which allows calculation of standard deviations.

Our approach and particularly our regulatory network selection is timely, considering the need to integrate the continuously evolving knowledge on leaf growth regulation (Kalve et al., 2014; Chaiwanon et al., 2016). An important limitation is our understanding of the specificity of hormone (auxin, cytokinin and gibberellin) metabolites and enzymes in the maize leaf, which led us to assign only one variable per set of active hormones of a family (Lor and Olszewski, 2015; Zürcher and Müller, 2016). This is also the case for enzyme isoforms for which only relative (qPCR derived) data are available. In absence of reliable absolute estimates of cellular metabolite concentrations and enzyme activities, our primary aim was to reproduce and predict their relative spatial and temporal molecular profiles. For leaf growth output, however, in most cases absolute values were used for fitting. In accordance with known data on maize leaf growth regulation, we made regulation of the cell division zone the main mechanism for altering leaf growth rate via those pathways. Indeed, a recent meta-analysis identified the regulation of the transition from cell division to cell expansion, in other words division zone size, as the key cellular mechanism that determines final size of plant organs (Gazquez and Beemster, 2017). Our simulations show that cell number regulation is a powerful way of leaf size regulation. Nelissen et al. (2012) demonstrated that the GA1 peak position is instrumental in locating the transition from division to expansion in the maize leaf and that modulating the GA1 peak affected the DZ size accordingly. This raises several compelling questions such as (i) how the GA1 peak is formed, (ii) how GA affects cell division (and cell expansion), and (iii) whether this effect is consistent with experimental growth and kinematic curves. By virtue of our modelling approach, we were able to shed more light on these questions. Whereas the data on the GA pathway enzyme transcript levels in wild type, UBI::GA20-OX-1 (Nelissen et al. 2012) appear to be qualitatively quite consistent with GA1 (and the GA8 inactivation product) peak changes, the question remains how underlying enzyme levels (activities) are regulated during leaf development. Using a knowledge-based model for regulation of expression of the principal pathway enzymes by auxin and cytokinin, allowed us to reconstruct both the spatial patterns of the enzyme and CDK activities (Fig. S5) and the resulting GA1 and GA8 peaks (Fig. 5, Fig. S5) in a growing leaf. In the model, GA1 influences cell cycle activity through DELLA breakdown. It was shown previously that shutting down GA biosynthesis or decoupling DELLA from GA regulation inhibits leaf growth. The resulting dwarf plants however still have residual growth regulation, which we attribute to auxin and cytokinin acting as necessary factors to support basal (slow) growth in a GA-independent way. Future experimental studies of spatial patterning of hormones under different abiotic or biotic stresses may reveal a more specific role for GA dependent growth regulation (Nelissen et al., 2018), but also point at the involvement of other signals that may explain effects on rates of cell expansion cell division (Avramova et al., 2015a; Rymen et al., 2007; Tardieu et al., 2000) that are not explained by the current model. Our analysis however shows that GA-dependent regulation with DELLA as a central regulator or signal integrator (Davière & Achard, 2016) on top of an auxin and cytokinin regulatory module provides a mechanism for fine tuning growth, by controlling the size of the division zone. By incorporating this regulation, our model can reproduce

experimental growth curves. Growth rate increase through higher GA levels works by increasing DZ size and CDK activity. This potentially also affects duration of growth, since it sustains CDK activity, unless this is balanced by compensatory catabolic activity. Indeed, the duration of leaf growth is relatively constant in controlled conditions for the studied lines, which suggested that GA influences growth rate rather than duration of growth. These simulations indicate that the absence of an effect of GA on the duration of growth results from a balance between stimulation of cell division by GA and increased growth inhibition due a compensatory growth inhibition from larger amount of mature tissue formed as a consequence of this.

The new experimental data on the evolution of hormone levels at the leaf base (Fig. 2) indicate that auxin and cytokinin supply decreases gradually. Based on the spatial data of auxin and cytokinin (2 days after leaf appearance), older tissue in more distal positions, contains progressively lower levels of those hormones. Although we cannot rule out a contribution of local biosynthesis, our observations suggest that these spatial gradients are a consequence of non-cell autonomous long-range (transport) of auxin and cytokinin at/to the leaf base. The advantage of non-cell-autonomous regulation has been pointed out before (De Vos et al., 2014). Clearly, the potential role of distant sources (shoot and root apices) and sinks of plant hormones, particularly younger leaves, provides a dynamic context and implicates the importance of plant architecture in resource allocation for growth regulation throughout the development of a leaf. Studies of mutants perturbed in auxin or cytokinin metabolism, transport or signalling could further support and refine their role in this context.

The concept that faster growth due to higher GA leads to faster (and earlier) decreases in growth rates led us to propose a feedback inhibition mechanism in which the leaf itself shuts down its growth, analogous to that observed in *Arabidopsis thaliana* (Andriankaja et al., 2012). Faster growth more quickly yields sufficient mature leaf tissue that signals meristematic tissue at the leaf base to stop growing via a long-range signal. This mechanism provides an explanation for the readily observed "back-yard" phenomenon that growth of grasses continues or is stimulated upon mowing. Inhibition of growth by light is relatively well studied in the context of shade avoidance, where the growth of plants that are shaded by (taller) neighbouring plants is stimulated, explaining for example the remarkable similarity in height of neighbouring crop plants in the field. A number of light receptors, responding to different clues have been identified. Of these, phytochromes primarily respond to changes in the (red) light spectrum, cryptochromes respond to levels of (blue) light and UVR encodes a specific receptor for UV-B radiation (Sessa *et al.*, 2018). Importantly, analogous to the implementation in our model, the signals induced by reception of shading by phytochromes and cryptochromes affect auxin homeostasis by regulation of synthesis, conjugation and catabolism, transport, perception and signalling (Iglesias *et al.*, 2018). Similarly, UV-B, detected by UVR8, provides a light signal that inhibits shade avoidance growth responses in *Arabidopsis thaliana* by inhibiting auxin and gibberellin signalling (Hayes et al., 2014). Our shading experiments suggest that light intensity and not spectrum trigger the observed growth inhibition and the observations on UV-B in *Arabidopsis* support the proposition that this signal feeds back to the auxin and/or GA metabolism controlling cell division in the growth zone. The growth response in the maize leaf provides an excellent basis for more detailed analysis of the auxin metabolism, transport and response as well as the impact of light signals from the mature part of the leaf to extend the details of the model beyond the scope of the higher level covered by the current work.

In conclusion, we developed a model capturing growth regulation in the monocotyledonous (maize) leaf, in which a two-layered structure reproduces the stable lay-out of the leaf growth axis (Division-Elongation-Mature), with auxin/cytokinin supplied at the leaf base driving a basal growth and determining leaf growth duration and GA providing a mechanism to control growth rates through division zone size control. This basic model explains observations of gene expression, metabolites and cellular growth processes and provides verifiable predictions, the most prominent of which is the presence of a negative feedback signal from the mature part of the leaf.

Acknowledgements

We thank Sevgi Oden for help with hormone analyses. This work was supported by a concerted research activity (GOA) research grant from the University of Antwerp, the European Research Council ERC Grant [339341-AMAIZE], and the Interuniversity Attraction Poles Program (IUAP P7/29 "MARS") initiated by the Belgian Science Policy Office. DD was funded by a return grant from BELSPO. HA is a postdoctoral researcher of the Research Foundation – Flanders (FWO; 12U8918N). The authors declare that they have no conflict of interest.

Author contributions:

DDV performed the modelling. HA, HN and EP performed experimental work. JB supervised the modelling. DDV, HN, DI and GB developed the model concept, discussed intermediate stages and wrote the manuscript.

Tables

Table 1. Overview of the model variables

Variable name	Explanation
CK	(Active) cytokinins (sum *c*-Z, *c/t*-ZR, iP, iPA, BAP)
AUX	Auxin (IAA)
GA1	Active gibberellin
GA8	Inactive 'downstream' gibberellin (catabolic product)
DELLA	DELLA growth regulating factors
GA20/3OX	Gibberellin anabolic complex (mainly GA20OX, GA3OX)
GA2OX	Gibberellin catabolic complex
CDK	Cyclin dependent kinase complex

Figures

Figure 1

Schematic representation of the regulatory wiring of signalling molecules involved in maize leaf growth regulation. Lines terminating with an arrow indicate stimulation or activation, lines terminating with a line indicate inhibition. The central regulatory axis with cytokinin (CK) and Auxin stimulating cell division through activation of cyclin dependent kinase (CDK) activity is coloured green. The gibberellic acid (GA) regulatory modul, including combined GA20/3 (GA20/3OX) oxidase activity producing the active GA1, GA2OX activity catalysing the catabolic inactivation of GA1 to the inactive GA8 and the DELLA protein inhibiting CDK activity, coloured orange. The blue area represents cross-talk between the cytokinin/auxin and GA modules.

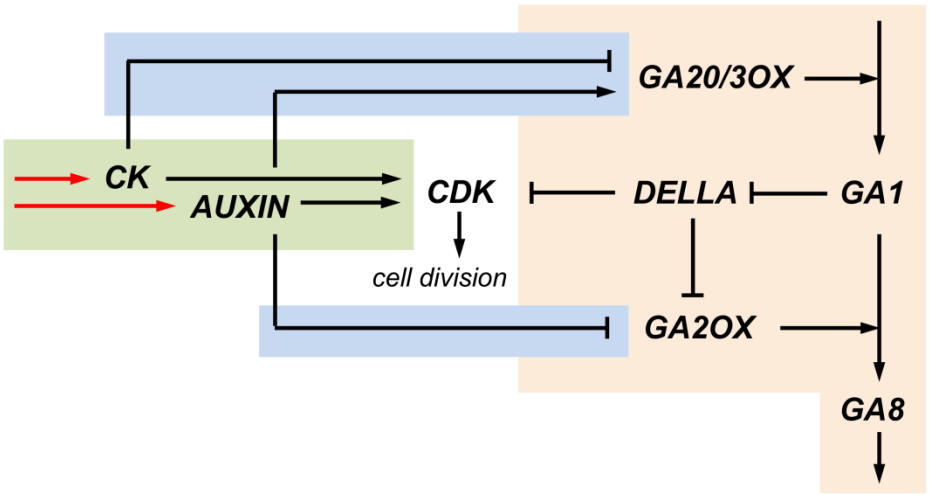

Figure 2

Simulation of the influx and measured hormone concentrations at the base of the maize leaf.

Comparison of measured (black dashed lines) and simulated (coloured lines) hormone concentrations at the leaf base. (A): measured auxin (IAA) concentration; (B): Sum of concentrations of (active) cytokinines measured (cZ, IPA, BAP, tZR, cZR; cf. Materials & Methods for full names). Individual cytokinin levels are shown in Fig. S2. Values for the experimental data represent averages +/- standard errors (n = 4).

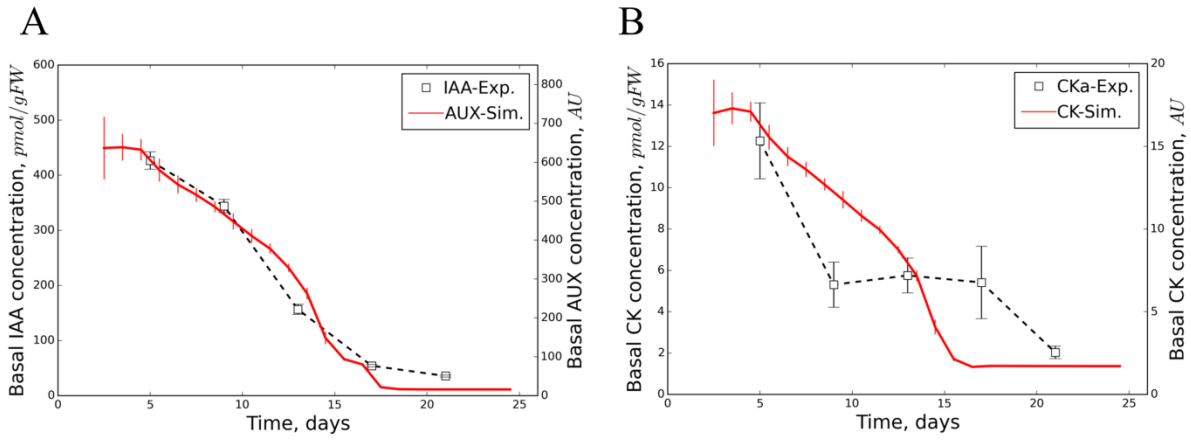

Figure 3.

Simulation of longitudinal Auxin and cytokinin distribution along the maize leaf growth zone.

(A) Experimentally measured cytokinin (t-Z; blue) and auxin (IAA; red) concentration along the maize leaf growth zone, 2 days after leaf appearance. Values represent averages +/- standard errors (n = 4). (B) Simulated CK (blue) and AUX (red) concentrations at day 6.75 (27 time-steps).

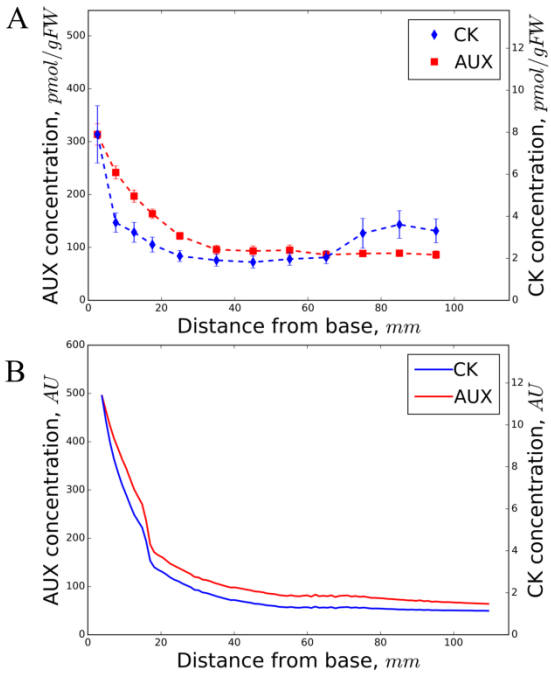

Figure 4

Simulation of longitudinal GA distribution along the maize leaf growth zone.

Measured (A-C; dashed lines) and simulated (D-F; full lines) spatial concentration (A, D-F) and expression (B, C) profiles at 2 days after leaf appearance of gibberellins (GA1, GA8) and important pathway enzymes (GA3OX, GA2OX) for wild type ('wt'; black), the GA20OX-1 overexpression line ('oe'; red), and the *dwarf3* mutant line ('dw'; blue). Measured values represent averages +/- SE (n = 4).

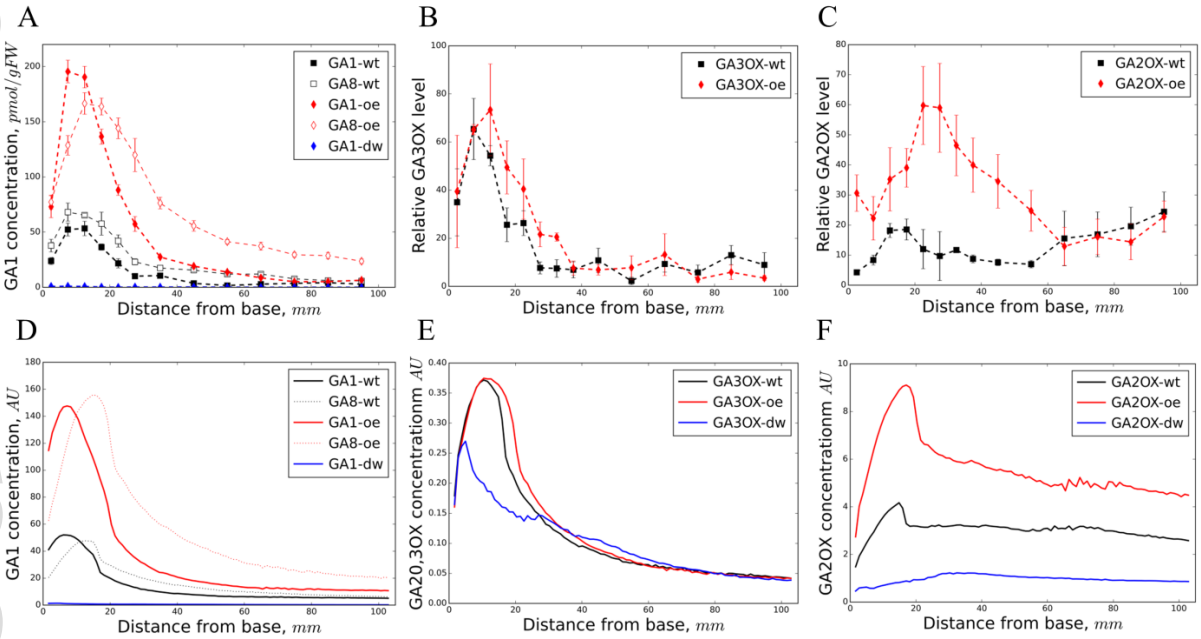

Figure 5

The evolution of hormone distribution patterns throughout the development of the maize leaf. 3D line plots showing the dynamics of spatial profiles from leaf growth simulations. (A) AUX (red) and CK (blue) concentrations scaled to the value of the most basal data point at the day of leaf appearance (0 days after leaf appearance). (B) GA1 (blue), GA8 (red), and DELLA concentrations (DELLA concentrations were multiplied by 4 to magnify the surface characteristics).

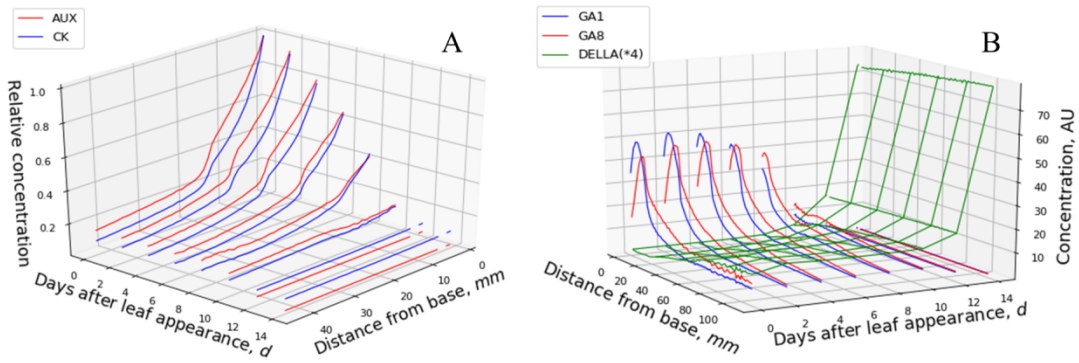

Figure 6

Simulating the effects of modulating GA production on maize leaf growth dynamics.

Average leaf length (A) and leaf elongation rate (LER, calculated as finite differences; B) for (10) simulation runs (with different random number seeds for the cell mechanics algorithm) of Wild Type (black), UBI::GA20-OX-1 (red) and *dwarf3* (blue) maize line models. The dashed line corresponds to the assumed day of leaf appearance in the simulation (after 19 time-steps). Values represent averages +/- standard deviations of 10 simulation datasets.

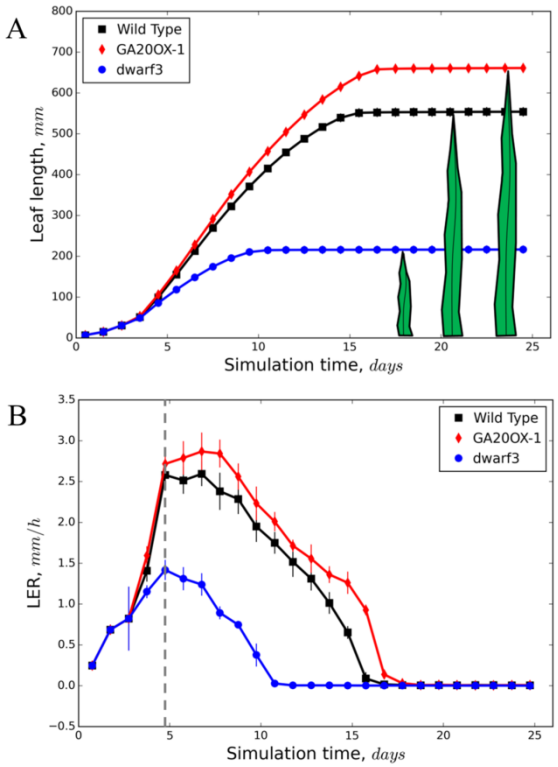

Figure 7

The effect of altered GA production on cell length profiles along the maize leaf growth zone.

Relative cell lengths (normalized to the initial (lattice) cell length) at 6.75 days (time step 27) based on simulations for the Wild Type (black), UBI::GA20-OX-1(red), and *dwarf3* (blue) models (with altered supply rates). Values represent averages +/- standard deviations of the (relative) cell lengths for 10 simulation runs per model and after binning the data in 3 mm intervals depending on the location of the cell centres relative to the leaf base.

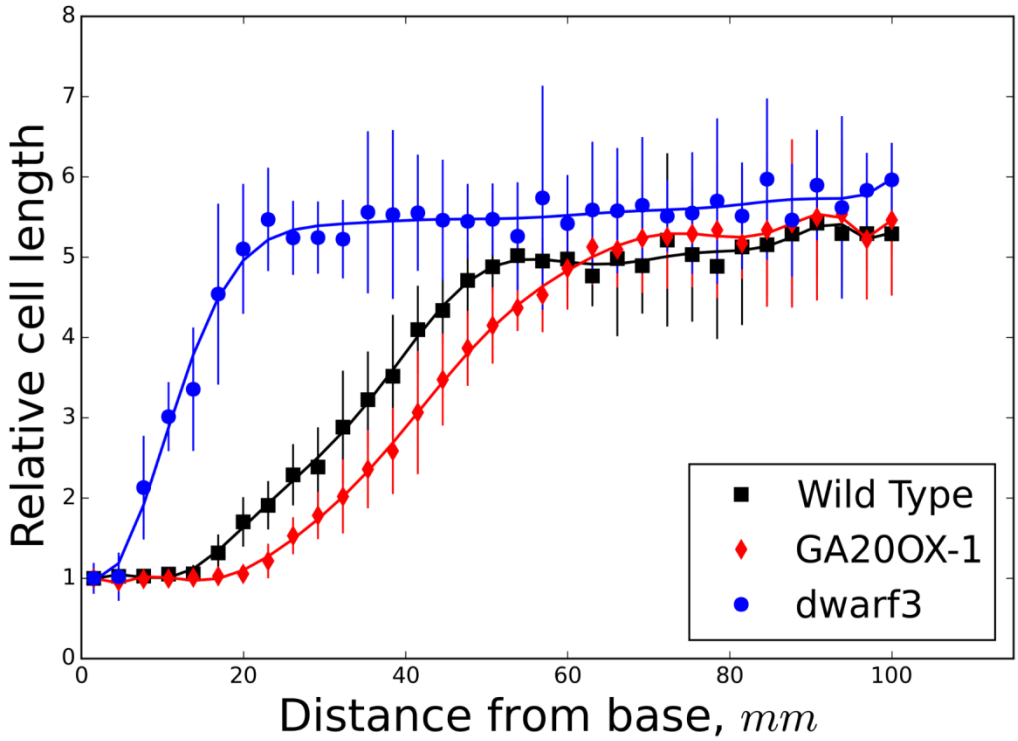

Figure 8

Predicted effect of feedback from mature part of the maize leaf on basal cytokinin and auxin supply.

Comparison of the wild type (black colour) (A) leaf length and (B) leaf elongation rate (LER) dynamics for simulations with the 'feedback model' with parameter KiM = 50 (red), 100 (green), and 200 (red). Values represent averages +/- standard deviations over 10 simulation runs. The dashed line represents the day of leaf appearance (19-time steps).

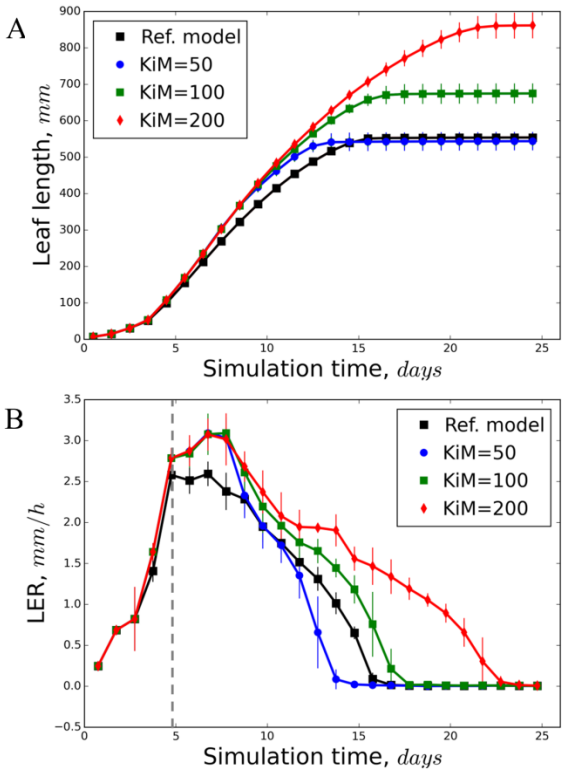

Figure 9

Experimentally removing the mature part of the leaf affects mature maize leaf size.

(A) Example leaves demonstrating the difference of the final length of the control leaf (right), to the reconstituted cut leaf (left), and the covered leaf (middle). Scale bar indicates 30cm. (B) The mean final leaf lengths for plants of control (n=19), cut (n=20) and covered (n=20) leaves, with standard errors and letters indicating significance ($p < 0.05$) from paired T-tests.

A

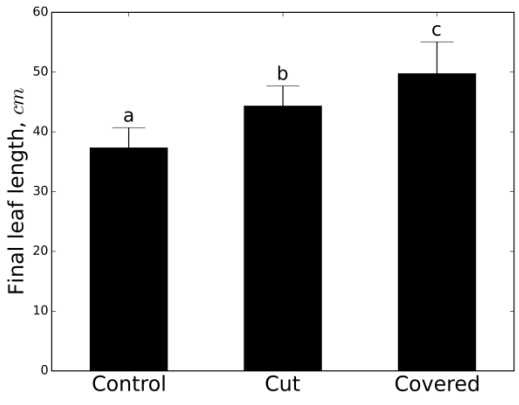

B

Figure 10.

Perturbing the feedback signal from the mature part of the maize leaf.

A. The effect of covering the leaf with aluminium foil, cutting the emerged mature part, reducing the light intensity with shade cloth and reducing evaporation with transparent plastic foil. B. Total number of cells and C. Mature cell length in leaves of which the mature part of the leaf is covered in different ways. D. The effect of covering the mature part of the leaf in different ways on meristem size at 3 days after emergence. Values are means +/- standard errors of at least 8 replicates and significant differences ($P<0.05$) are indicated by different letters.

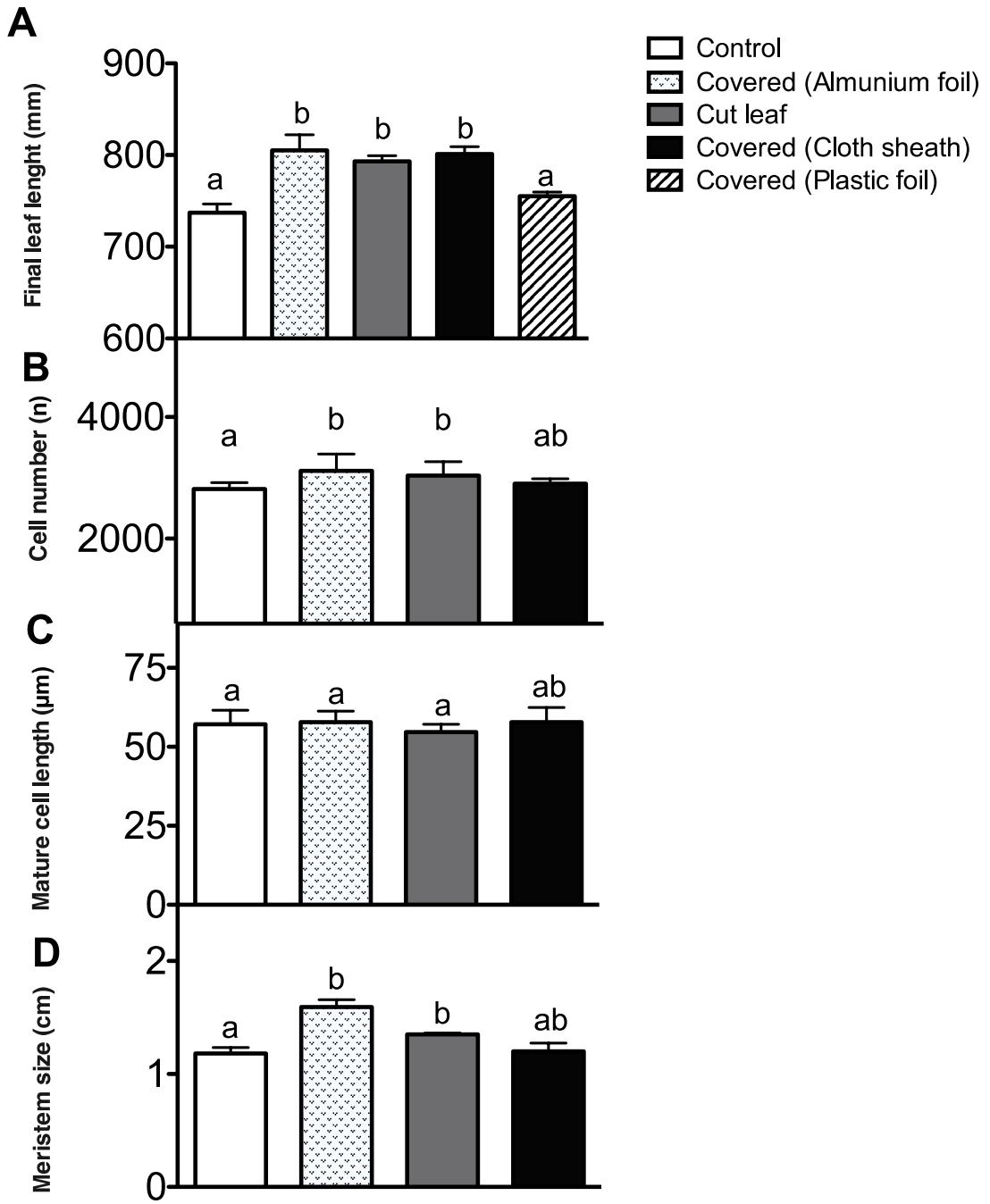

References

Achard P, Gusti A, Cheminant S, Alioua M, Dhondt S, Coppens F, Beemster GTS, Genschik P. 2009. Gibberellin signaling controls cell proliferation rate in Arabidopsis *Current Biology* 19: 1188-1193.

Andriankaja, M., Dhondt, S., De Bodt, S., Vanhaeren, H., Coppens, F., De Milde, L., Muhlenbock, P., Skirycz, A., Gonzalez, N., Beemster, G.T.S., et al. (2012). Exit from Proliferation during Leaf Development in *Arabidopsis thaliana*: A Not-So-Gradual Process. Developmental Cell 22, 64-78.

Avramova, V., AbdElgawad, H., Zhang, Z., Fotschki, B., Casadevall, R., Vergauwen, L., Knapen, D., Taleisnik, E., Guisez, Y., Asard, H., et al. (2015a). Drought induces distinct growth response, protection and recovery mechanisms in the maize leaf growth zone. Plant physiology 169, 1382 - 1396.

Avramova V, Sprangers K, Beemster GTS. (2015b) The Maize Leaf: Another Perspective on Growth Regulation. Trends Plant Sci. Dec;20(12):787-97.

Balzan S, Johal GS, Carraro N. (2014) The role of auxin transporters in monocots development.Front Plant Sci. Aug 15;5:393. doi: 10.3389/fpls.2014.00393. eCollection 2014.

Baute J, Herman D, Coppens F, De Block J, Slabbinck B, Dell'Acqua M, Pe ME, Maere S, Nelissen H, Inze D (2015) Correlation analysis of the transcriptome of growing leaves with mature leaf parameters in a maize RIL population. Genome Biol 16: 168.

Beemster, G.T.S., and Baskin, T.I. (2000). Stunted Plant 1 mediates effects of cytokinin, but not of auxin, on cell division and expansion in the root of Arabidopsis. Plant physiology 124, 1718-1727.

Beemster GTS, Masle J (1996) The role of apical growth around the time of leaf initiation in determining leaf width at maturity in wheat seedlings (*Triticum aestivum*.L.) with impeded roots. Journal of Experimental Botany 47: 1679-1688.

Ben-Zvi D, Barkai N (2010) Scaling of morphogen gradients by an expansion-repression integral feedback control. Proc Natl Acad Sci U S A. Apr 13; 107(15): 6924–6929. doi: 10.1073/pnas.0912734107

Bolle C. 2004. The role of GRAS proteins in plant signal transduction and development. Planta 218, 683–692.

Caldeira CF, Bosio M, Parent B, Jeanguenin L, Chaumont F, Tardieu F. 2014. A hydraulic model is compatible with rapid changes in leaf elongation under fluctuating evaporative demand and soil water status. *Plant Physiol* 164(4): 1718-1730.

Chaiwanon J, Wang W, Zhu JY, Oh E, Wang ZY. (2016) Information Integration and Communication in Plant Growth Regulation. Cell. Mar 10;164(6):1257-1268. doi: 10.1016/j.cell.2016.01.044

Claeys H, Skirycz A, Maleux K, Inzé D. (2012) DELLA signaling mediates stress-induced cell differentiation in Arabidopsis leaves through modulation of anaphase-promoting complex/cyclosome activity. Plant Physiol.. Jun;159(2):739-47. doi: 10.1104/pp.112.195032.

Davière JM, Achard P. (2016) A Pivotal Role of DELLAs in Regulating Multiple Hormone Signals. Mol Plant. Jan 4;9(1):10-20. doi: 10.1016/j.molp.2015.09.011.

De Vos D, Van Petegem F, Remaut H, Legrain C, Glansdorff N, Van Beeumen JJ. (2004) Crystal structure of T state aspartate carbamoyltransferase of the hyperthermophilic archaeon Sulfolobus acidocaldarius. J Mol Biol. Jun 11;339(4):887-900.

De Vos D, Xu Y, Hulpiau P, Vergauwen B, Van Beeumen JJ. (2007) Structural investigation of cold activity and regulation of aspartate carbamoyltransferase from the extreme psychrophilic bacterium *Moritella profunda*. J Mol Biol. Jan 12;365(2):379-95.

De Vos, D., Dzhurakhalov, A., Draelants, D., Bogaerts, I., Kalve, S., Prinsen, E., Vissenberg, K., Vanroose, W., Broeckhove, J., and Beemster, G.T. (2012) Towards mechanistic models of plant organ growth. J. Exp. Bot. 63, 3325-3337.

De Vos, D., Vissenberg, K., Broeckhove, J., and Beemster, G.T. (2014) Putting theory to the test: which regulatory mechanisms can drive realistic growth of a root? *PLoS Comput. Biol.* 10:e1003910.

De Vos D, Dzhurakhalov A, Stijven S, Klosiewicz P, Beemster GTS, Broeckhove J. (2017) Virtual Plant Tissue: Building Blocks for Next-Generation Plant Growth Simulation. Front Plant Sci. May 4;8:686. doi: 10.3389/fpls.2017.00686. eCollection 2017.

Dudits D, Abrahám E, Miskolczi P, Ayaydin F, Bilgin M, Horváth GV. (2011) Cell-cycle control as a target for calcium, hormonal and developmental signals: the role of phosphorylation in the retinoblastoma-centred pathway. Ann Bot. 107(7):1193-202. doi: 10.1093/aob/mcr038.

Fina, R. Casadevall, H. AbdElgawad, E. Prinsen, M. Markakis, G. Beemster, P. Casati, (2017) UV-B inhibits leaf growth through changes in Growth Regulating Factors and gibberellin levels, Plant Physiol. 174(2): 1110 – 1126.

Fleishon S, Shani E, Ori N, Weiss D. (2011) Negative reciprocal interactions between gibberellin and cytokinin in tomato. New Phytol. May;190(3):609-17. doi: 10.1111/j.1469-8137.2010.03616.x.

Frigerio M, Alabadi D, Perez-Gomez J, Gracia-Cacel L, Phillips AL, Hedden P, Blazquez MA (2006) Transcriptional regulation of gibberellin metabolism genes by auxin signaling in Arabidopsis. Plant Physiol 142: 553–563

Gázquez A, Beemster GTS. (2017) What determines organ size differences between species? A meta-analysis of the cellular basis. New Phytol. Jul;215(1):299-308. doi: 10.1111/nph.14573.

Grieneisen VA, Xu J, Maree AF, Hogeweg P, Scheres B. (2007). Auxin transport is sufficient to generate a maximum and gradient guiding root growth. *Nature* 449(7165): 1008-1013.

Hartig K, Beck E. (2006) Crosstalk between auxin, cytokinins, and sugars in the plant cell cycle.Plant Biol (Stuttg). May;8(3):389-96.

Hayes S, Velanis CN, Jenkins GI, Franklin KA (2014) UV-B detected by the UVR8 photoreceptor antagonizes auxin signaling and plant shade avoidance. Proc Natl Acad Sci U S A 111: 11894-11899.

Hodgman, TC and Ajmera, I. (2015) The successful application of systems approaches in plant biology. Prog. Biophys. Mol. Biol. 117, 59-68.

Hopkins, WG and Hüner, NPA (2008) Introduction to Plant Physiology. Wiley, New Jersey, USA. 4th edition, ISBN: 978-0-470-24766-2.

Iglesias MJ, Sellaro R, Zurbriggen MD, Casal JJ (2018) Multiple links between shade avoidance and auxin networks. J Exp Bot 69: 213-228.

Kalve, S., De Vos, D., and Beemster, G.T.S. (2014). Leaf development: a cellular perspective. Frontiers in Plant Science 5, 362.

Lor VS, Olszewski NE. (2015) GA signalling and cross-talk with other signalling pathways. Essays Biochem. 58:49-60. doi: 10.1042/bse0580049.

Merks, R.M.H., Van de Peer, Y., Inzé, D., and Beemster, G.T.S. (2007). Canalization without flux sensors: a traveling-wave hypothesis. Trends in Plant Science 12, 384-390.

Moore S, Zhang X, Mudge A, Rowe JH, Topping JF, Liu J, Lindsey K (2015) Spatiotemporal modelling of hormonal crosstalk explains the level and patterning of hormones and gene expression in *Arabidopsis thaliana* wild-type and mutant roots New Phytol. Sep; 207(4): 1110–1122. doi: 10.1111/nph.13421.

Nelissen H, Gonzalez N, Inze D (2016) Leaf growth in dicots and monocots: so different yet so alike. Curr Opin Plant Biol 33: 72-76.

Nelissen H, Rymen B, Jikumaru Y, Demuynck K, Van Lijsebettens M, Kamiya Y, Inzé D, Beemster GTS. (2012) A local maximum in gibberellin levels regulates maize leaf growth by spatial control of cell division. Curr Biol. Jul 10;22(13):1183-7.

Nelissen H, Sun XH, Rymen B, Jikumaru Y, Kojima M, Takebayashi Y, Abbeloos R, Demuynck K, Storme V, Vuylsteke M, De Block J, Herman D, Coppens F, Maere S, Kamiya Y, Sakakibara H, Beemster GTS, Inzé D. (2018) The reduction in maize leaf growth under mild drought affects the transition between cell division and cell expansion and cannot be restored by elevated gibberellic acid levels. Plant Biotechnol 16: 615 - 627. doi: 10.1111/pbi.12801.

O'Neill DP, Ross JJ (2002) Auxin regulation of the gibberellin pathway in Arabidopsis. Plant Physiol 130: 1974–1982.

O'Neill DP, Davidson SE, Clarke VC, Yamauchi Y, Yamaguchi S, Kamiya Y, Reid JB, Ross JJ. (2010) Regulation of the gibberellin pathway by auxin and DELLA proteins. Planta. Oct;232(5):1141-9. doi: 10.1007/s00425-010-1248-0.

Pacifici E, Polverari L, Sabatini S. (2015) Plant hormone cross-talk: the pivot of root growth. J Exp Bot. Feb;66(4):1113-21. doi: 10.1093/jxb/eru534

Perilli, S., Di Mambro, R., and Sabatini, S. (2012). Growth and development of the root apical meristem. Curr. Opin. Plant Biol. 15, 17–23. doi: 10.1016/j.pbi.2011.10.006.

Perrot-Rechenmann C. (2010) Cellular responses to auxin: division versus expansion. Cold Spring Harb Perspect Biol. May;2(5):a001446. doi: 10.1101/cshperspect.a001446.

Rymen, B., Fiorani, F., Kartal, F., Vandepoele, K., Inzé, D., and Beemster, G.T.S. (2007). Cold Nights Impair Leaf Growth and Cell Cycle Progression in Maize through Transcriptional Changes of Cell Cycle Genes. Plant Physiol. 143, 1429-1438.

Rymen B, Coppens F, Dhondt S, Fiorani F, Beemster GT. (2010) Kinematic analysis of cell division and expansion. Methods Mol Biol. 655:203-27. doi: 10.1007/978-1-60761-765-5_14.

Sessa G, Carabelli M, Possenti M, Morelli G, Ruberti I (2018) Multiple Pathways in the Control of the Shade Avoidance Response. Plants (Basel) *7*(4), 102; https://doi.org/10.3390/plants7040102.

Stals H, Inze D 2001. When plant cells decide to divide. Trends Plant Sci 6:359–364.

Sun X, Cahill J, Van Hautegem T, Feys K, Whipple C, Novak O, Delbare S, Versteele C, Demuynck K, De Block J, Storme V, Claeys H, Van Lijsebettens M, Coussens G, Ljung K, De Vliegher A, Muszynski M, Inze D, Nelissen H (2017) Altered expression of maize PLASTOCHRON1 enhances biomass and seed yield by extending cell division duration. Nat Commun 8: 14752.

Swarup R, Kramer EM, Perry P, Knox K, Leyser HM, Haseloff J, Beemster GTS, Bhalerao R, Bennett MJ. 2005. Root gravitropism requires lateral root cap and epidermal cells for transport and response to a mobile auxin signal. *Nature Cell Biology* 7(11): 1057-1065.

Tardieu, F., Reymond, M., Hamard, P., Granier, C., and Muller, B. (2000). Spatial distributions of expansion rate, cell division rate and cell size in maize leaves: a synthesis of the effects of soil water status, evaporative demand and temperature. Journal of experimental botany 51, 1505-1514.

Ubeda-Tomas S, Swarup R, Coates J, Swarup K, Laplaze L, Beemster GTS, Hedden P, Bhalerao R, Bennett MJ. 2008. Root growth in Arabidopsis requires gibberellin/DELLA signalling in the endodermis. *Nature Cell Biology* 10(5): 625 - 628.

Úbeda-Tomás S, Dyson RJ, Middleton AM, Hodgman TC, Owen MR, Jensen OE, Bennett MJ, King JR. (2012) Growth-induced hormone dilution can explain the dynamics of plant root cell elongation. Band LR, Proc Natl Acad Sci U S A. May 8;109(19):7577-82.

Verbelen JP, De Cnodder T, Le J, Vissenberg K, Baluska F. (2006) The Root Apex of Arabidopsis thaliana Consists of Four Distinct Zones of Growth Activities: Meristematic Zone, Transition Zone, Fast Elongation Zone and Growth Terminating Zone. Plant Signal Behav 1: 296-304.

Weiss, D., and Ori, N. (2007). Mechanisms of cross talk between gibberellin and other hormones. Plant Physiol. 144, 1240–1246. doi: 10.1104/pp.107.100370

Weston DE, Elliott RC, Lester DE, Rameau C, Reid JB, Murfet IC, Ross JJ (2008) The pea (*Pisum sativum*) DELLA proteins LA and CRY are important regulators of gibberellin synthesis and root growth. Plant Physiol 147:199–205.

Xu H, Liu Q, Yao T, Fu X. (2014) Shedding light on integrative GA signaling. Curr Opin Plant Biol. Oct;21:89-95. doi: 10.1016/j.pbi.2014.06.010.

Yue R, Tie S, Sun T, Zhang L, Yang Y, Qi J, Yan S, Han X, Wang H, Shen C. (2015) Genome-wide identification and expression profiling analysis of ZmPIN, ZmPILS, ZmLAX and ZmABCB auxin transporter gene families in maize (*Zea mays* L.) under various abiotic stresses. PLoS One. Mar 5;10(3):e0118751. doi: 10.1371/journal.pone.0118751. eCollection 2015.

Zentella R, Zhang Z, Park M, Thomas SG, Endo A, Murase K, Fleet CM, Jikumaru Y, Nambara E, Kamiya Y, Sun T-p (2007) Global analysis of DELLA direct targets in early gibberellin signaling in Arabidopsis. Plant Cell 19:3037–3057

Zürcher E, Müller B. (2016) Cytokinin Synthesis, Signaling, and Function--Advances and New Insights. Int Rev Cell Mol Biol.;324:1-38. doi: 10.1016/bs.ircmb.2016.01.001.

Supporting Information